Stem Cell Reports
Report
ISSCR
OPEN ACCESS

# Generation of a Motor Nerve Organoid with Human Stem Cell-Derived Neurons

Jiro Kawada,[1] Shohei Kaneda,[1] Takaaki Kirihara,[1,2] Asif Maroof,[3,4,5] Timothée Levi,[1] Kevin Eggan,[3,4] Teruo Fujii,[1] and Yoshiho Ikeuchi[1,2,*]

[1]Institute of Industrial Science, The University of Tokyo, Tokyo 153-8505, Japan
[2]Department of Chemistry and Biotechnology, Graduate School of Engineering, The University of Tokyo, Tokyo 113-8656, Japan
[3]Department of Stem Cell and Regenerative Biology, and Harvard Stem Cell Institute, Harvard University, Cambridge, MA 02138, USA
[4]Stanley Center for Psychiatric Research, Broad Institute of MIT and Harvard, Cambridge, MA 02142, USA
[5]Present address: Department of Biology, University of Texas San Antonio, TX 78249, USA
*Correspondence: yikeuchi@iis.u-tokyo.ac.jp
https://doi.org/10.1016/j.stemcr.2017.09.021

## SUMMARY

During development, axons spontaneously assemble into a fascicle to form nerves and tracts in the nervous system as they extend within a spatially constrained path. However, understanding of the axonal fascicle has been hampered by lack of an *in vitro* model system. Here, we report generation of a nerve organoid composed of a robust fascicle of axons extended from a spheroid of human stem cell-derived motor neurons within our custom-designed microdevice. The device is equipped with a narrow channel providing a microenvironment that facilitates the growing axons to spontaneously assemble into a unidirectional fascicle. The fascicle was specifically made with axons. We found that it was electrically active and elastic and could serve as a model to evaluate degeneration of axons *in vitro*. This nerve organoid model should facilitate future studies on the development of the axonal fascicle and drug screening for diseases affecting axon fascicles.

## INTRODUCTION

During development, neurons spontaneously assemble to build organized structures and functional circuits in various parts of the nervous system. A fascicle of axons is one of the major structural motifs often observed in the nervous system, e.g., the peripheral nerves, corticospinal tract, and corpus callosum (Ahsan et al., 2007; Stewart, 2003). Previous studies have shown that an axonal fascicle is formed as growing axons follow and gather along the preceding "pioneer axon" through axo-axonal interactions *in vivo*; however, further details of the mechanism of this process are yet to be clarified (Raper and Mason, 2010). Importantly, axon fascicles are often damaged by neurodegenerative diseases (Ito et al., 2016). For instance, previous studies suggest that amyotrophic lateral sclerosis disrupts axonal maintenance mechanisms, including the protein transportation system, thereby causing specific elimination of motor neurons (Alami et al., 2014; Bilsland et al., 2010; LaMonte et al., 2002; Morfini et al., 2009). Although numerous insights into the developmental and pathophysiological mechanisms have been derived from studies on single axons in dissociated 2D culture, we have little insight into fascicles of axons due to the lack of *in vitro* culture systems.

Human stem cell-derived neurons could provide a promising platform in drug discovery and the development of therapeutics for devastating neurological disorders, and they have been extensively studied for understanding neuronal development, functions, and diseases (Sances et al., 2016; Shi et al., 2012; Sterneckert et al., 2014). Since it is increasingly apparent that proper multi-cellular organization and microenvironment are critical for physiological modeling of development and diseases of the nervous system, *in vitro* three-dimensional brain "organoid" culture systems have been proposed to provide improved systems that more accurately represent multi-cellular structures (Lancaster et al., 2013; Sasai, 2013). The emerging technology currently relies on cell-intrinsic, self-assembly mechanisms to form tissue morphology, and few extrinsic environmental factors are considered. By developing methods that can form organoids representing specific parts of the nervous system, we would be able to model development and diseases of specific neuronal structures and circuitry.

In this study, we developed a method for the formation of a nerve organoid composed of a fascicle of axons extended from a spheroid of human stem cell-derived motor neurons. By providing a spatially confined environment in a microchannel, axons spontaneously assembled into a unidirectional fascicle within the microchannel. The resultant fascicle of axons can be subjected to various examinations, including morphological, electrical, and physical analyses. This nerve organoid model mimics development and dysfunction of a human motor nerve, thus potentially serving as a platform for high-throughput screening.

## RESULTS

### Generation of Nerve Organoids

To build an organoid mimicking developing nerve tissue, we employed a strategy that allowed the neurons to follow the cell-intrinsic axon growth and fasciculation programs

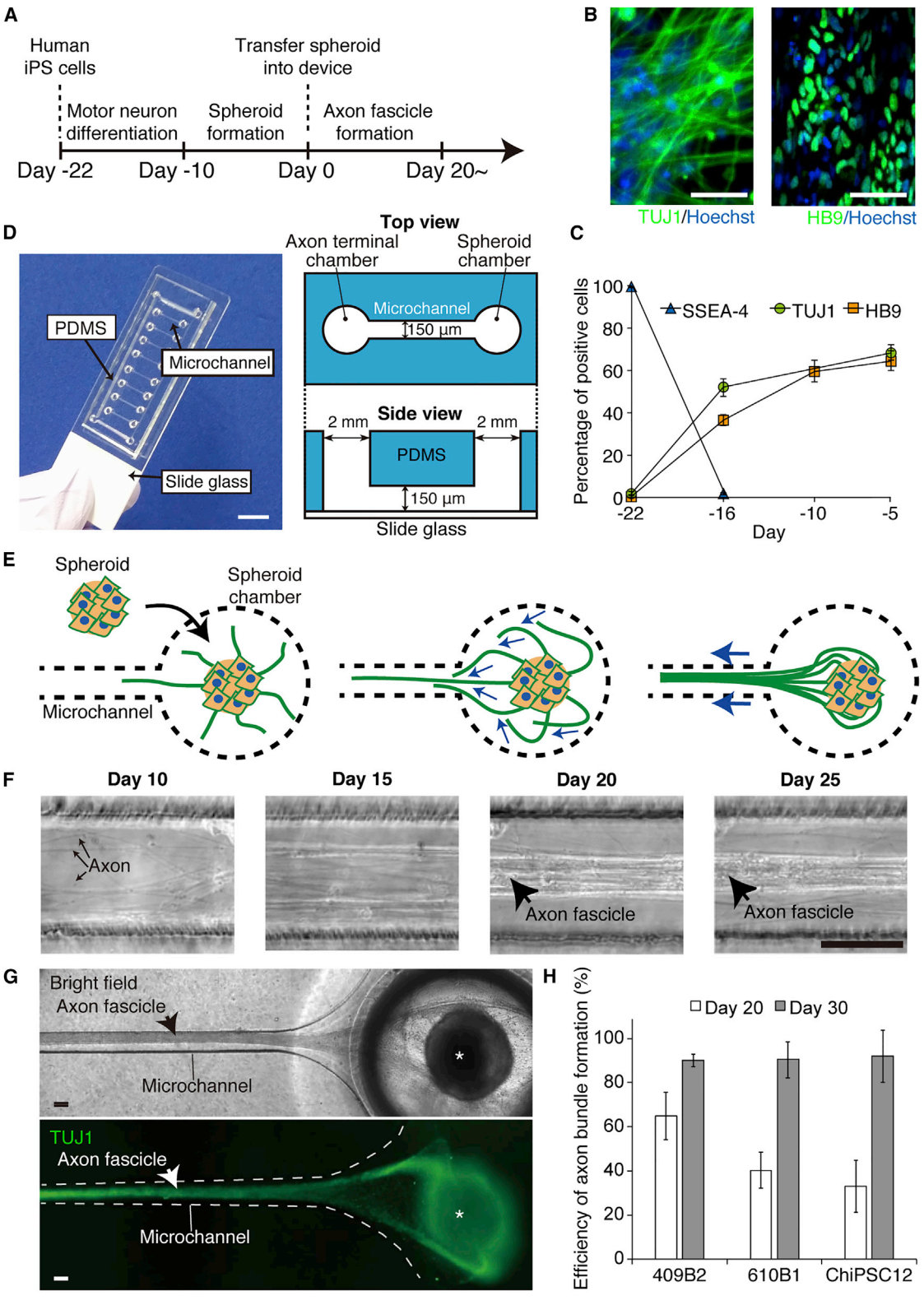


*(legend on next page)*

with minimal intervention. We first differentiated human induced pluripotent stem cells (hiPSCs) into spinal motor neurons for 12 days (Figure 1A). The neurons were then assembled into a spheroid for 10 days within a low-adhesive culture vessel. During these steps, pluripotent stem cell marker SSEA-4-positive cells were decreased and TUJ1-positive neuronal cells were increased correspondingly (Figures 1B and 1C). Importantly, more than 60% of cells expressed the motor neuron marker HB9 during the differentiation procedure (Figures 1B and 1C). The spheroid was transferred into a custom-made culture device for axon fascicle formation. The culture microdevice contains a chamber receiving a spheroid, a microchannel for axon fascicle formation, and a target chamber accommodating axon terminals (Figure 1D). Neurons spontaneously extended axons out from the spheroid in the chamber. As a portion of axons grew into the microchannel, other axons followed and extended into the microchannel. Consequently, the axons spontaneously formed a single, straight, and unidirectional fascicle within the microchannel after culturing the spheroid for about 20 days (Figures 1E–1G). The resulting structure, which we refer to as a nerve organoid, consists of two mutually connected parts: an axon fascicle and a spheroid of neurons. The efficiency of axon fascicle formation was over 90% at day 30 in three hiPSC lines derived from different individuals (Figure 1H), demonstrating that the nerve organoid formation process is robust and reliable.

## Recapitulation of Motor Nerve Organization

After axon fascicles were formed (>20 days in the microdevice), nerve organoids were collected from the culture vessels, which allowed for various assessments of the organoids (Figure 2A). Whole-mount immunostaining of the collected organoid revealed that the axon fascicle was immunoreactive for axonal protein TAU1, while nuclear staining signals were absent in the axon fascicle (Figure 2A). In contrast, the spheroid was both TAU1 immunoreactive and nuclear staining positive. Further immunohistological analyses of cryosections confirmed that the fascicle contained axonal protein TAU1 and presynaptic protein SYNAPSIN1, but not nuclei or dendritic protein MAP2 (Figures 2B and 2C). Consistent with the histological observations, a western blotting analysis of cell lysates of physically separated spheroids and axon fascicles revealed that TAU1 and presynaptic protein SYNAPTOPHYSIN were present in the axon fascicle lysate, but MAP2 and nuclear envelope protein NUCLEOPORIN were not (Figure 2D). These data indicate the fascicle structure formed in the microchannel contained axons, but not cell bodies or dendrites, and demonstrated successful organization of the axon fascicle spatially separated from the spheroid.

To address the identity of the motor neurons in the organoid, we stained for neuronal marker TUJ1 and the motor neuron marker SMI32 (Figures 2E and 2F). We observed that the majority of the cells are TUJ1-positive neurons. Importantly, about 50% of the cells in the organoids were SMI32-positive motor neurons. A minor fraction of cells were GFAP-positive astrocytes, and almost no cells were positive for neural stem cell marker NESTIN and oligodendrocyte marker O4. We employed scanning electron microscopy to observe the surface of the fascicle. The surface appeared to be unidirectionally assembled with numerous fibers (Figure 2G). To assess the internal structure, we analyzed the cross-section morphology of the fascicle at a higher magnification using transmission electron microscopy (TEM) (Figure 2H). This revealed that numerous axons were contained within the fascicle. Cross-sections of well-organized cytoskeletal fibers, including microtubules, were observed within the axons. In addition, the axons were directly contacting each other and packed tightly within the fascicle, which demonstrated that the

**Figure 1. Nerve Organoid Formation in a Microdevice**

(A) Schematic timeline of nerve organoid generation from human induced pluripotent stem cells (hiPSCs). hiPSCs were differentiated into motor neuron for 12 days, and the neurons were subjected to spheroid formation for 10 days. After these steps, the spheroids were transferred to microdevices at day 0. Axon fascicles were formed after around 20–30 days of culture in the microdevice.

(B) Immunofluorescent images of differentiated cells immunostained with TUJ1 antibody (left) and HB9 antibody (right) at day 5.

(C) Percentage of SSEA-4-, TUJ1-, and HB9-positive cells during the differentiation process. The error bar denotes the SE of means of values acquired from three independent experiments.

(D) A photograph (left) and schematic drawings (right) of the microdevice.

(E) Schematic drawings of spontaneous axon fascicle formation in the microdevice, illustrating the growth of axons from the spheroid within a chamber (left), axons following the preceding axon in the microchannel (middle), and axon fascicle formation and growth (right).

(F) Representative time-lapse images of axons and an axon fascicle within a microchannel.

(G) A bright-field representative image of a nerve organoid (top) and a fluorescent image of the same organoid immunolabeled with TUJ1 (bottom) within a microdevice. Asterisks indicate a spheroid comprising the nerve organoid.

(H) Success rate of axon fascicle formation using three independent hiPSC lines. An assembled bundle of axons with a diameter of over 25 μm was counted as an axon fascicle. The error bar denotes the SE of means of values acquired from three independent experiments. A total of 90 samples were analyzed. Scale bars, 10 μm (B), 100 μm (F and G), and 4 mm (D).

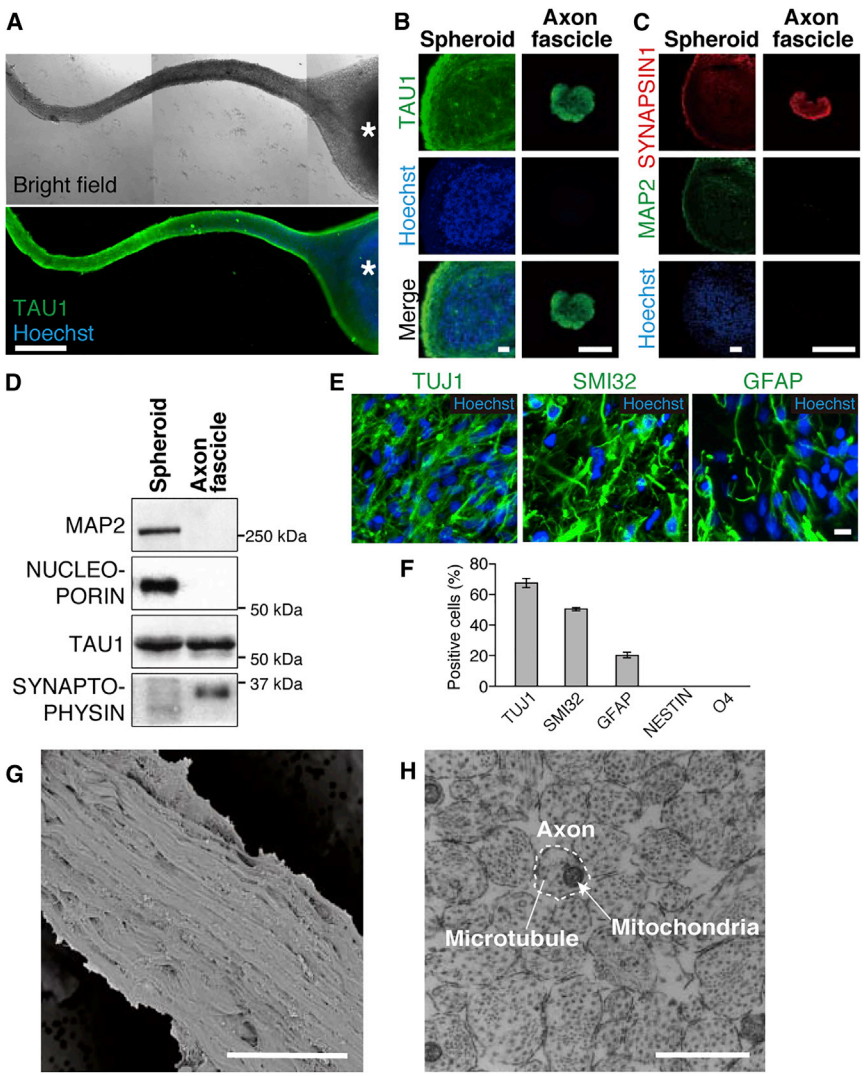


**Figure 2. Characterization of Nerve Organoids**

(A) Representative images of a nerve organoid collected from the culture device. Bright-field (top) and fluorescent immunolabeling with TAU1 antibody (bottom). Asterisks indicate neuronal spheroid within a nerve organoid.

(B) Images of cryosections from spheroid (left) and axon fascicle (right) of a nerve organoid stained with TAU1 antibody (top), with Hoechst 33342 (middle), and merged (bottom).

(C) Images of cryosections from spheroid (left) and axon fascicle (right) of a nerve organoid stained with SYNAPSIN1 antibody (top), MAP2 antibody (middle), and Hoechst 33342 (bottom).

(D) Western blotting analysis of spheroid and axon fascicle lysates.

(E) Cryosections of spheroid within a nerve organoid immunostained with TUJ1 antibody (left), SMI32 antibody (middle), and with GFAP antibody (right).

(F) Percentage of TUJ1-, SMI32-, GFAP-, NESTIN-, and O4-positive cells by cell counting. The error bar denotes the SE of means of values acquired from three independent organoids.

(G) A representative scanning electron microscopy image of an axon fascicle.

(H) A representative transmission electron microscopy image of an axon fascicle cross-section. Scale bars, 500 μm (A), 50 μm (B and C), 10 μm (E), 20 μm (G), and 800 nm (H).

axons were assembled into a fascicle within the nerve organoid.

## Electrophysiological and Physical Property of Nerve Organoid

Next, we assessed the electrophysiological functionality of the neurons in the nerve organoid. Using a microelectrode array system, we recorded alterations of field potential near cell bodies of neurons in a nerve organoid. We observed spontaneous activity (Figures 3A and 3B), suggesting that the neurons in the organoid are functional. We observed synchronous activity from multiple electrodes contacting the organoid (Figure 3B), indicating that the neurons formed a functional network. To address the functionality of the axonal fascicle, we applied electrical stimulation to a spheroid compartment of a nerve organoid and assessed if electrical activity was propagated to the axon fascicle using calcium indicator dye (Figures 3C and 3D, Movie S1). Both spheroid and axon fascicle in the organoid responded to electrical stimulation. Importantly, the axon fascicle did not respond to electrical stimulation after it was separated from the spheroid where electric stimulation was applied. These data suggest that the nerve organoid is functionally active, and its axon fascicle conducts electrical activity.

Since the nerve fascicles were physically robust, we were able to pinch and grab them manually with forceps (Figure 3E). To evaluate its mechanical properties in the axon fascicles, we assessed the extension of the axon fascicle and applied force (Onoe et al., 2013) (Figures 3F and 3G; Movie S2). Tensile load-extension curves of three fascicles were assessed (Figure 3H). This result indicates that the fascicles were elongated in a linear manner against tensile load. A cross-section of a stretched fascicle was analyzed using TEM (Figure 3I), and a number of microtubules in the

obtained images were counted (Figure 3J). The counting revealed that the number of microtubules was decreased by the mechanical stresses. The results obtained here indicate that the formed fascicles can serve as a unique platform for assessing the physical properties of an axon fascicle, and can be further applied for regenerative studies of acute physical damages to axons and nerves.

### Nerve Organoids Model Neurodegeneration

Next, we used the nerve organoid to model neuronal damage and degeneration. Hydrogen peroxide ($H_2O_2$) treatment was employed to model the pathogenesis of oxidative stress-mediated neurodegenerative disease (Figure 4A). At day 30, we treated a nerve organoid with $H_2O_2$ for 3 hr, and then continued to culture it in fresh medium for 2 days. Observation of the organoid by bright-field microscopy revealed that the surface texture of the $H_2O_2$-treated nerve organoid became rough compared with the control (Figure 4B). The surface change in response to $H_2O_2$ treatment was confirmed with higher-magnification observation of the surface of the axon fascicle with scanning electron microscopy (Figure 4C). By texture analysis of the bright-field images of axon fascicles, we found that the roughness of the surface was significantly increased by the $H_2O_2$ treatment (Figure 4D). Immunostaining with TAU1 antibody further revealed that the axon fascicle had lost its linear and fibrous appearance (Figure 4E). By analyzing the TAU1-immunostaining images of the axon fascicles with a directional quantification software package, we found that the apparent directionality of axons within the nerve organoid was substantially reduced upon $H_2O_2$ treatment (Figures 4F and 4G). These data demonstrate that the nerve organoid can be used to model neuronal disorders caused by stress, and that texture analysis and directionality analysis provide unique quantitative indices for the health and quality of the nerve organoid. Since these measurements can be easily performed, they would be suitable for high-throughput chemical compound screening for neurological diseases affecting axons.

## DISCUSSION

In summary, we developed a method for the construction of a nerve model from human stem cell-derived motor neurons. We demonstrated that the method presented here yielded a robust fascicle consisting of axons organized in a unidirectional structure. We successfully characterized the electrical and mechanical properties of the axon fascicles. Further, we modeled chemical stress on the nerve and provided easy methods to quantify the degeneration, suggesting that the nerve organoid can serve as a useful tool for compound evaluation and drug screening.

Compartmentalization of axons from other parts of neurons in *in vitro* cultures has been achieved in several well-characterized methods. Conventionally, an explant method of dorsal root ganglion neurons has been used widely to obtain or observe physically separated axons extending outward from other parts of the neurons. More recently, microdevices and porous filters were used to isolate axons by excluding cell bodies from a defined compartment with sufficiently small windows that only axons, but not cell bodies, can pass through. Although the microdevices and filters improve the purity of axons, they often yield a significantly reduced number of axons compared with the explant method. In our method, we achieved compartmentalization of axons from soma and dendrites by simply forming a spheroid with hiPSC-derived motor neurons and allowing axons to extend from the spheroid into a microchannel. Neurons in the spheroid exhibit limited motility, and cell bodies are only occasionally seen in the proximal part of the axon fascicle in the channel. By dissecting the axon fascicles, we were able to obtain high-quality axon lysates sufficient for western blotting analysis. We did not detect nuclear or dendritic proteins in the axonal lysate, demonstrating that our method efficiently separated axons from cell bodies and dendrites.

To test if growing neurons in a 3D spheroid is necessary for axon fascicle formation within the microdevice, we grew neurons in 2D inside the microdevice (data not shown). By enlarging the chamber to accommodate an equivalent number of cells, we could occasionally observe formation of axon fascicles similar to those formed from a spheroid of neurons. However, the efficiency of axon fascicle formation was low, and thus, was far less robust and reliable compared with the method presented in the current manuscript.

By only aligning axons in one orientation in a microchannel, we achieved assembly of axon fascicles. Alignment of axons presumably facilitates axo-axonal interactions to efficiently promote the formation of axon fascicles in the microdevice. In conventional two-dimensional culture of neurons, fasciculation of axons is occasionally observed but generally considered to be a product of insufficient interaction between neurons and culture surface, which in turn allows interaction between axons. To promote axon fascicle formation by avoiding excessive interaction between axons and culture surface, we coated the surface inside the microchannel with extracellular matrix proteins (Matrigel) instead of conventionally used synthetic polymer poly-L-lysine or ornithine. The axons formed a fascicle in a microdevice coated with Matrigel, but axons separately adhered to the culture surface and did not form a fascicle in a poly-L-lysine-coated microdevice (data not shown). These observations imply that

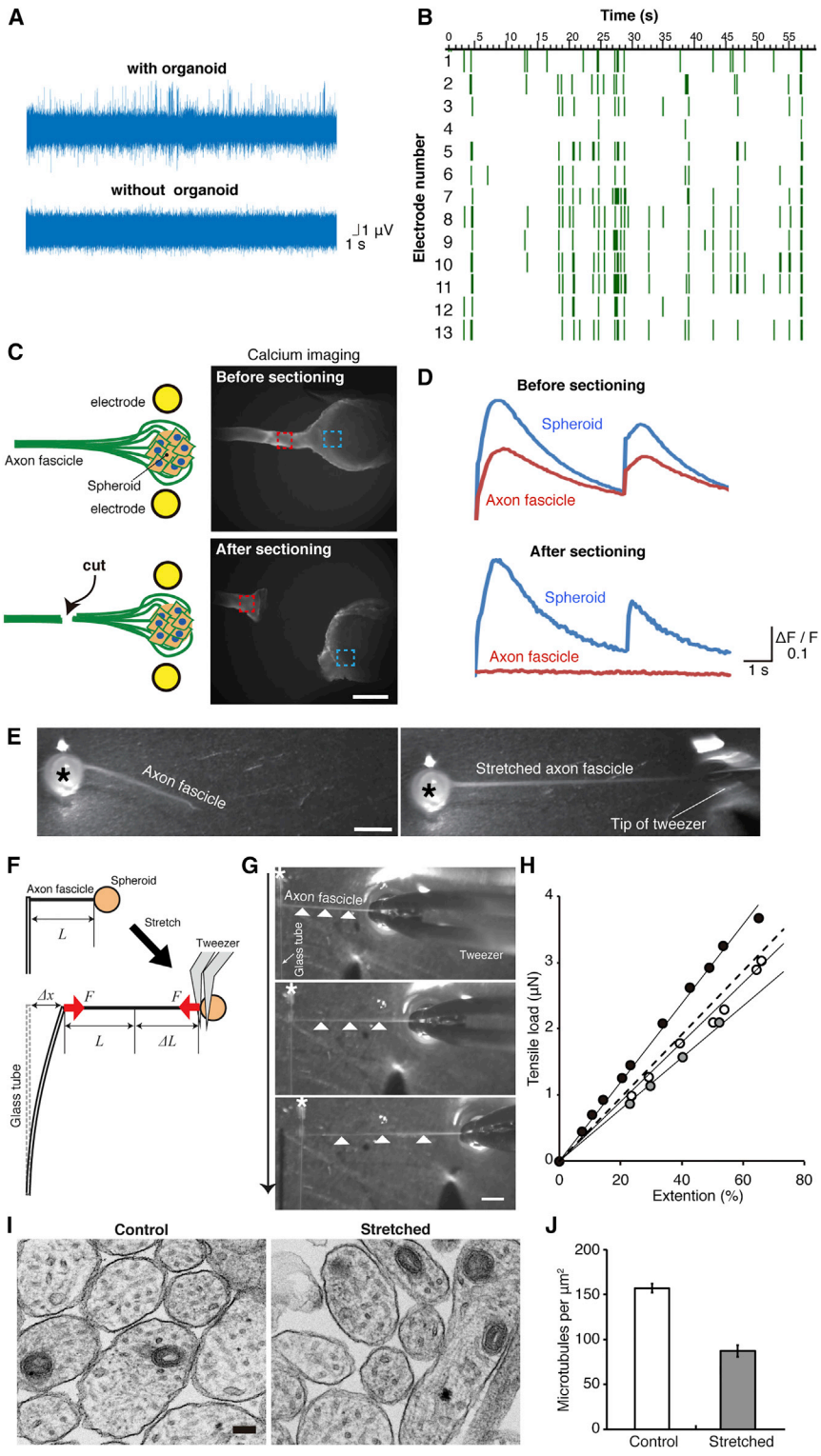


**Figure 3. Electrophysiological and Physical Properties of Nerve Organoids**

(A) Monitoring of the spontaneous electrical activity in an organoid using a microelectrode array. Representative filtered signal obtained from an electrode with (top) and without (bottom) an organoid.

(B) Representative spike raster plot showing synchronized neuronal network activity. Signals were thresholded at 3 μV (3 times more than noise amplitude).

(C) Schematics and representative images of Fluo-4-AM-based calcium imaging with electrical stimulation before (top) and after (bottom) sectioning the base of an axon fascicle.

(D) Monitoring of fluorescent intensities of Fluo-4-AM with electrical stimulation before (top) and after (bottom) sectioning the axon fascicle. Fluorescent intensity was obtained from blue (spheroid) and red (axon fascicle) dotted area in (C).

(E) An axon fascicle is pinched and elongated by tweezers. Asterisks denote spheroids.

(F) Schematic drawings of experimental setup for mechanical strength measurement.

(G) Representative sequential images of a measurement. Asterisks indicate the tip of the glass tube and triangles show points dividing the elongated axon fascicle into four.

(H) Typical tensile load-elongation curves.

(I) TEM images of cross-sections of stretched axon fascicle (right) and non-stretched control (left).

(J) Number of microtubules per unit area ($\mu m^2$) within axons was counted with the TEM images of cross-sections of axon fascicles. Significantly fewer microtubules were observed in the stretched axon fascicles than in untreated controls (Student's t test; $p < 0.05$). Scale bars, 500 μm (C), 1 mm (E and G), and 100 nm (I). See also Movies S1 and S2.

strength of interaction between axons and between axon and surrounding matrix or cells is strictly controlled *in vivo* to achieve formation of axon fascicles and nerves.

The nerve organoid assembly method reported here provides an important step in modeling axon fascicles present in the nervous system. We have assembled a nerve

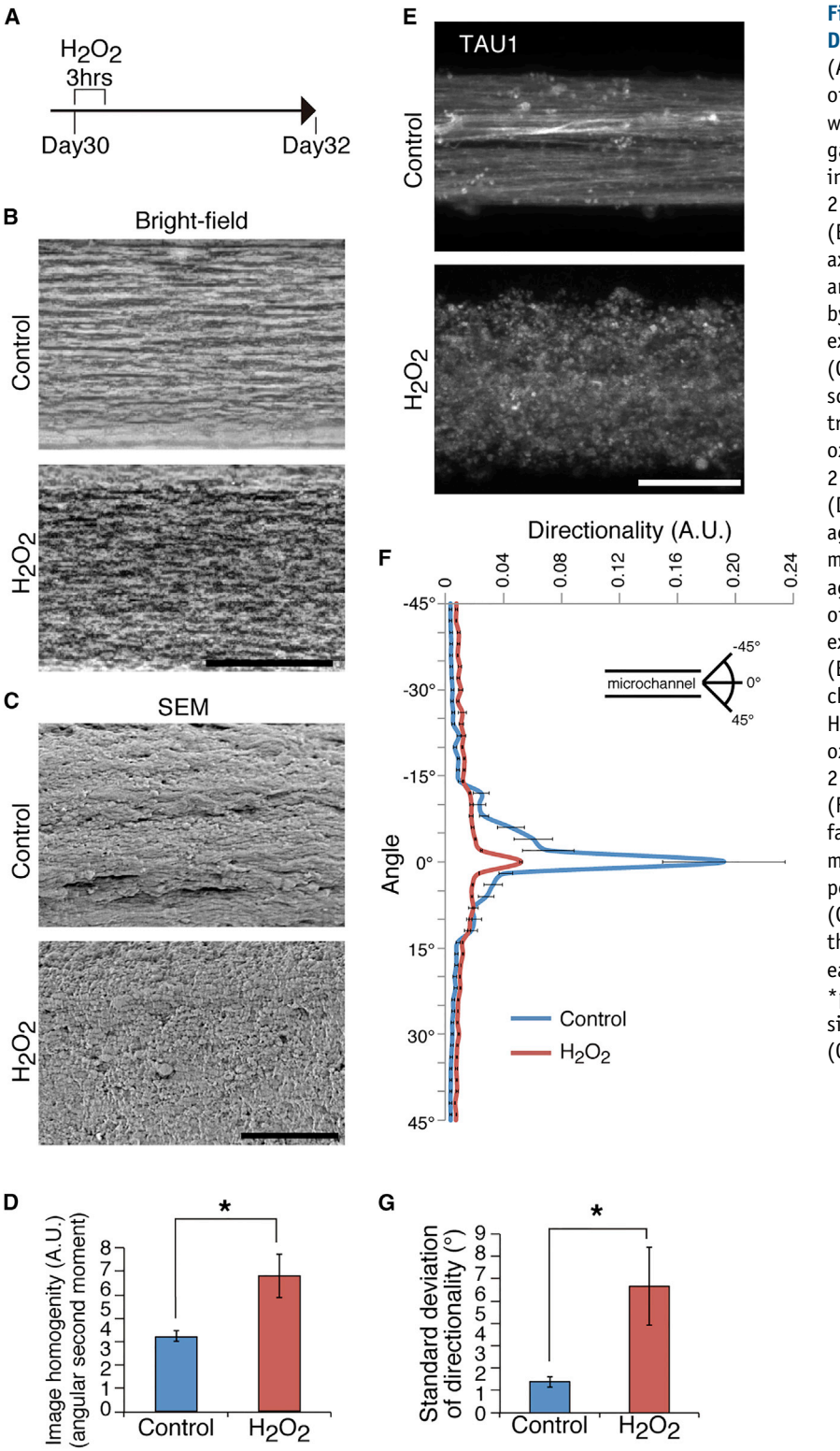


**Figure 4. Oxidative Stress-Induced Nerve Degeneration Model**

(A) Experimental timeline for $H_2O_2$ treatment of nerve organoids. At day 30, organoids were treated with $H_2O_2$ for 3 hr. Control organoids were exposed to fresh normal media instead of $H_2O_2$-containing media. After 2 days, the nerve organoids were evaluated.

(B) Representative bright-field images of axon fascicles without $H_2O_2$ treatment (top), and after induction of oxidative stress by 10 μM $H_2O_2$ for 3 hr at 2 days before examination (bottom).

(C) Representative scanning electron microscopy images of axon fascicles without $H_2O_2$ treatment (top), and after induction of oxidative stress by 10 μM $H_2O_2$ for 3 hr at 2 days before examination (bottom).

(D) The texture analysis of bright-field images of axon fascicles. The angular second movement represents homogeneity of images. The error bar denotes the SE of means of values acquired from three independent experiments (n = 3 for each group).

(E) Representative TAU1 immunohistochemistry images of axon fascicles without $H_2O_2$ treatment (top), and after induction of oxidative stress by 10 μM $H_2O_2$ for 3 hr at 2 days before examination (bottom).

(F) The directionality analysis of the axon fascicles. The error bar denotes the SE of means of values acquired from three independent experiments (n = 3 for each group).

(G) Average of SD of the directionalities from three independent experiments (n = 3 for each group).

*$p < 0.05$ (Student's t test) and statistically significant. Scale bars, 100 μm (B), 10 μm (C), and 100 μm (E).

organoid using motor neurons derived from hiPSCs, which models the peripheral motor nerve. It will be interesting to apply this method to other types of neurons to model axon fascicles in the nervous system, e.g., the sensory nerve, corticospinal tract, and corpus callosum. Further, it will be interesting to provide postsynaptic target cells so that neurons can interact through synaptic connections. In addition, the nerve organoid can serve as a basic building block for *in vitro* connectivity modeling in "brain-on-a-chip" applications by connecting the axon fascicle with neurons or non-neuronal target cells. At this point in model development, the nerve organoid presented in this study did not contain myelin or an outer sheath (perineurium) that would naturally form after the development of the axon fascicle (Nave and Werner, 2014; Piña-Oviedo and Ortiz-Hidalgo, 2008). We believe that the current method shows the way for further development of the nerve model and axon fascicle structures by amending methods to provide myelination and sheath formation in future studies.

## EXPERIMENTAL PROCEDURES

### Culture Device Fabrication

The culture devices were fabricated by the standard molding process (Hosokawa et al., 1999). The mold master was fabricated with an SU-8 2100 photoresist (MicroChem) using photolithography. We made microchannels 150 ± 10 μm in height. The photoresist was spin coated at 2,000 rpm on a silicon wafer. The photoresist-coated silicon wafer was baked at 95°C for 30 min. Then the photoresist was exposed to UV with the glass mask. After UV exposure, the silicon wafer was baked again at 95°C for 5 min. Finally, the wafer was developed using propylene glycol monomethylether. Poly(dimethylsiloxane) (PDMS, Dow Corning Toray) was poured on the mold and baked at 75°C for 2 hr. The PDMS chip was peeled from the mold, and then the culture chambers were punched using a 2-mm diameter biopsy trepan (Natsume Seisakusho). The PDMS chip was bonded to a glass bottom using oxygen plasma (Hosokawa et al., 1999). The culture device was sterilized using an autoclave (121°C for 15 min).

### iPS Cell Culture and Differentiation

409B2 and 610B1 hiPSC lines were provided by Kyoto University through RIKEN BioResource center cell bank (HPS0076 and HPS0331) (Okita et al., 2011, 2013). ChiPSC12 hiPSC line was purchased (Takara Bio). The iPS cells were cultured on a Vitronectin (VTN-N, Thermo Fisher Scientific)-coated dish with Essential 8 Medium (Thermo Fisher Scientific) to maintain the undifferentiated state. The motor neurons were differentiated by the previously described protocol with slight modifications (Chambers et al., 2009). hiPSCs were dissociated with Accutase (Millipore), and seeded on Matrigel (growth factor reduced, Corning, BD Biosciences)-coated dish with Essential 8 Medium with ROCK inhibitor Thiazovivin (1 μM, Tocris), and cultured until they reached 80% confluence. As an initial differentiation medium, we used DMEM/F12 medium (Thermo Fisher Scientific) supplemented with 15% Knockout Serum Replacement (Thermo Fisher Scientific), GlutaMAX (Thermo Fisher Scientific), non-essential amino acid solution (Thermo Fisher Scientific), 10 μM SB-431542 (Sigma-Aldrich), and 100 nM LDN-193189 (Sigma-Aldrich) for the following 2 days. The medium was gradually switched to N2 medium (neurobasal medium supplemented with N2 supplement, GlutaMAX, and penicillin-streptomycin; Thermo Fisher Scientific) over the following 8 days. During this period, cells were treated with 1 μM retinoic acid (Sigma-Aldrich), 1 μM Smoothened Agonist (SAG, Calbiochem), 4 μM SU5402 (Sigma-Aldrich), and 5 μM DAPT (Sigma-Aldrich). The differentiated cells were dissociated by Accutase and seeded in a low-adhesion V-bottom 96-well plate (Sumitomo Bakelite) for 10 days to generate spheroids.

### Formation of Motor Nerve Organoids

The culture devices were coated with Matrigel. The coating solution was replaced by motor neuron culture medium (B27 medium supplemented with 1 μM retinoic acid and 1 μM SAG), and then the spheroids were transferred into the culture device. Half of the culture medium was replaced with fresh medium every 4 days. Typically, 20–30 days after spheroids are transferred into the device, an axon fascicle forms within the microchannel.

### Collection of Nerve Organoids from Culture Devices

Nerve organoids were collected from the culture microdevice by manually injecting 200 μL PBS from the axon terminal chamber after brief treatment with Accutase for 2 min. To collect axon fascicles and spheroids separately for biochemical analyses, nerve organoids were dissected manually by cutting through the PDMS device with a razor blade. After collecting spheroids, axon fascicles were collected from the device by pipetting PBS into the microchannels. Experimental Procedures for characterization of nerve organoids are described in detail in Supplemental Experimental Procedures.

## SUPPLEMENTAL INFORMATION

Supplemental Information includes Supplemental Experimental Procedures and two movies and can be found with this article online at https://doi.org/10.1016/j.stemcr.2017.09.021.

## AUTHOR CONTRIBUTIONS

J.K., E.K., T.F., and Y.I. designed the study; J.K., S.K., T.K., and A.M. conducted cellular and molecular experiments; T.K. and T.L. performed and analysed the MEA recordings; J.K., S.K., T.K., and Y.I. wrote the manuscript; S.K. and T.K. contributed equally.

## ACKNOWLEDGMENTS

We thank Mss. Sanae Furusho, Shoko Wada, and Atsumi Ozaki (JASCO International Co., Ltd.) for assistance with scanning electron microscopic analyses. We thank Drs. Naoko Yoshie and Hirotaka Ejima for providing equipment for sputtering. We thank Dr. Agnes Tixier-Mita for providing equipment for MEA recording. We thank Mr. Romain Beaubois and Dr. Hiroaki Onoe for assisting with the MEA recordings and mechanical characterization, respectively. We also thank Dr. Yusuke Hirabayashi and the members of Ikeuchi laboratory for helpful discussion and critical reading of

the manuscript. This study was supported by the Japan Society for the Promotion of Science (JSPS) Grants-in-Aid for Scientific Research 26890008 and 17H05661 (to Y.I.) and by a Sentei Kenkyu grant at the Institute of Industrial Science (to Y.I.). Patent applications based on the presented research have been filed. The patents are planned to be licensed to Jiksak Bioengineering, Inc., which was founded by Jiro Kawada, the first author of this paper.

Received: February 7, 2017
Revised: September 25, 2017
Accepted: September 25, 2017
Published: October 26, 2017

## REFERENCES

Ahsan, M., Riley, K.L., and Schubert, F.R. (2007). Molecular mechanisms in the formation of the medial longitudinal fascicle. J. Anat. *211*, 177–187.

Alami, N.H., Smith, R.B., Carrasco, M.A., Williams, L.A., Winborn, C.S., Han, S.S., Kiskinis, E., Winborn, B., Freibaum, B.D., Kanagaraj, A., et al. (2014). Axonal transport of TDP-43 mRNA granules is impaired by ALS-causing mutations. Neuron *81*, 536–543.

Bilsland, L.G., Sahai, E., Kelly, G., Golding, M., Greensmith, L., and Schiavo, G. (2010). Deficits in axonal transport precede ALS symptoms in vivo. Proc. Natl. Acad. Sci. USA *107*, 20523–20528.

Chambers, S.M., Fasano, C.A., Papapetrou, E.P., Tomishima, M., Sadelain, M., and Studer, L. (2009). Highly efficient neural conversion of human ES and iPS cells by dual inhibition of SMAD signaling. Nat. Biotechnol. *27*, 275–280.

Hosokawa, K., Fujii, T., and Endo, I. (1999). Handling of picoliter liquid samples in a poly(dimethylsiloxane)-based Microfluidic device. Anal. Chem. *71*, 4781–4785.

Ito, Y., Ofengeim, D., Najafov, A., Das, S., Saberi, S., Li, Y., Hitomi, J., Zhu, H., Chen, H., Mayo, L., et al. (2016). RIPK1 mediates axonal degeneration by promoting inflammation and necroptosis in ALS. Science *353*, 603–608.

LaMonte, B.H., Wallace, K.E., Holloway, B.A., Shelly, S.S., Ascaño, J., Tokito, M., Van Winkle, T., Howland, D.S., and Holzbaur, E.L. (2002). Disruption of dynein/dynactin inhibits axonal transport in motor neurons causing late-onset progressive degeneration. Neuron *34*, 715–727.

Lancaster, M.A., Renner, M., Martin, C.A., Wenzel, D., Bicknell, L.S., Hurles, M.E., Homfray, T., Penninger, J.M., Jackson, A.P., and Knoblich, J.A. (2013). Cerebral organoids model human brain development and microcephaly. Nature *501*, 373–379.

Morfini, G.A., Burns, M., Binder, L.I., Kanaan, N.M., LaPointe, N., Bosco, D.A., Brown, R.H., Brown, H., Tiwari, A., Hayward, L., et al. (2009). Axonal transport defects in neurodegenerative diseases. J. Neurosci. *29*, 12776–12786.

Nave, K.A., and Werner, H.B. (2014). Myelination of the nervous system: mechanisms and functions. Annu. Rev. Cell Dev. Biol. *30*, 503–533.

Okita, K., Matsumura, Y., Sato, Y., Okada, A., Morizane, A., Okamoto, S., Hong, H., Nakagawa, M., Tanabe, K., Tezuka, K., et al. (2011). A more efficient method to generate integration-free human iPS cells. Nat. Methods *8*, 409–412.

Okita, K., Yamakawa, T., Matsumura, Y., Sato, Y., Amano, N., Watanabe, A., Goshima, N., and Yamanaka, S. (2013). An efficient nonviral method to generate integration-free human-induced pluripotent stem cells from cord blood and peripheral blood cells. Stem Cells *31*, 458–466.

Onoe, H., Okitsu, T., Itou, A., Kato-Negishi, M., Gojo, R., Kiriya, D., Sato, K., Miura, S., Iwanaga, S., Kuribayashi-Shigetomi, K., et al. (2013). Metre-long cell-laden microfibres exhibit tissue morphologies and functions. Nat. Mater. *12*, 584–590.

Piña-Oviedo, S., and Ortiz-Hidalgo, C. (2008). The normal and neoplastic perineurium: a review. Adv. Anat. Pathol. *15*, 147–164.

Raper, J., and Mason, C. (2010). Cellular strategies of axonal pathfinding. Cold Spring Harb. Perspect. Biol. *2*, a001933.

Sances, S., Bruijn, L.I., Chandran, S., Eggan, K., Ho, R., Klim, J.R., Livesey, M.R., Lowry, E., Macklis, J.D., Rushton, D., et al. (2016). Modeling ALS with motor neurons derived from human induced pluripotent stem cells. Nat. Neurosci. *19*, 542–553.

Sasai, Y. (2013). Next-generation regenerative medicine: organogenesis from stem cells in 3D culture. Cell Stem Cell *12*, 520–530.

Shi, Y., Kirwan, P., Smith, J., Robinson, H.P., and Livesey, F.J. (2012). Human cerebral cortex development from pluripotent stem cells to functional excitatory synapses. Nat. Neurosci. *15*, 477–486.

Sterneckert, J.L., Reinhardt, P., and Schöler, H.R. (2014). Investigating human disease using stem cell models. Nat. Rev. Genet. *15*, 625–639.

Stewart, J.D. (2003). Peripheral nerve fascicles: anatomy and clinical relevance. Muscle Nerve *28*, 525–541.